Structural Characterization of Horseradish Peroxidase Using EXAFS Spectroscopy. Evidence for Fe=O Ligation in Compounds I and II

James E. Penner-Hahn,*[1a,b] Kim Smith Eble,[1c,d] Thomas J. McMurry,[1b] Mark Renner,[1e] Alan L. Balch,[1e] John T. Groves,[1b,f] John H. Dawson,*[1c] and Keith O. Hodgson*[1a]

Contribution from the Department of Chemistry, The University of Michigan, Ann Arbor, Michigan 48109-1055, the Department of Chemistry, The University of South Carolina, Columbia, South Carolina 29208, the Department of Chemistry, University of California, Davis, California 95616, and the Department of Chemistry, Stanford University, Stanford, California 94305. *Received May 5, 1985*

Abstract: Extended X-ray absorption fine structure spectroscopy has been utilized to determine the structural environment of the heme iron sites in horseradish peroxidase compounds I and II. For comparison, analogous studies have been undertaken on putative ferryl (Fe^{IV}=O) porphyrin model compounds and on crystallographically characterized Cr^{IV}=O and Cr^{V}≡N porphyrins. In a preliminary communication, we suggested that a short ca. 1.6 Å Fe–O bond is present in the high valent forms of both the enzyme and the synthetic porphyrins. The present work demonstrates unambiguously that a short, ca. 1.64 Å, Fe–O bond length is present both in HRP compounds I and II and in their synthetic analogues. This structure is consistent only with an oxo-ferryl (Fe=O) complex as the active oxygen species in horseradish peroxidase. The structural details, their implications for heme protein mediated oxygen activation, and the difference between our results and those recently published by other workers (Chance, B.; Powers, L.; Ching, Y.; Poulos, T.; Schonbaum, G. R.; Yamazaki, I.; Paul, K. G. *Arch. Biochem. Biophys.* **1984**, *235*, 596–611) are discussed.

The transport and activation of dioxygen by heme proteins is a subject of continuing interest. For proteins which activate dioxygen, the prototype being cytochrome P-450, the general mechanism is believed to involve transient formation of an activated iron–oxo species.[2,3] The crystal structure of ferric P-450 has recently appeared,[4] however, the putative Fe(O) intermediate for this enzyme has not yet been isolated, and if isolated, it is unlikely to be sufficiently stable to permit crystallographic structure determination. However, the active oxygen species in P-450 is generally believed to be structurally similar to the high-valent intermediates formed during the catalytic cycle of the peroxidase enzymes.[3] As part of a continuing program to characterize the mechanism of heme-mediated oxygen activation,[5,6] we have undertaken an X-ray absorption spectroscopy (XAS)[7] study of the high-valent intermediates formed during the catalytic cycle of horseradish peroxidase (HRP).

Horseradish peroxidase is a heme-containing enzyme that catalyzes the oxidation of phenolic substrates, utilizing hydrogen peroxide as the ultimate electron acceptor. The resting form of HRP contains a high-spin ferric heme. During the catalytic cycle

Scheme I

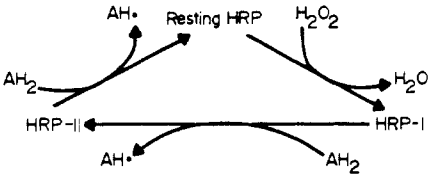

(see Scheme I), HRP is initially oxidized by two electrons to a green species known as compound I (HRP-I). One-electron reduction of HRP-I yields the red species known as compound II (HRP-II), which retains one oxidizing equivalent above the resting enzyme.

The intermediates in the HRP reaction cycle have been subjected to extensive physical and chemical characterization.[8–10] The resting enzyme contains a five-coordinate heme, with the fifth coordination site occupied by an axial imidazole ligand.[4,11–13] HRP-I is two oxidation equivalents above ferric iron and therefore formally contains Fe^{V}. Magnetic susceptibility measurements[14] indicate that there are three unpaired electrons ($S = {}^3/_2$) in HRP-I. This has been explained by ferromagnetic coupling of low-spin Fe^{IV} ($S = 1$) to a porphyrin π-cation radical ($S = {}^1/_2$). Consistent with this assignment is the similarity of the optical spectrum of HRP-I and those of synthetic porphyrin π-cations.[15] Investigations of HRP-I by NMR[16] and ENDOR[17] as well as iterative extended Hückel (IEH) calculations[18] all favor the π-

(1) (a) Stanford University. (b) University of Michigan. (c) University of South Carolina. (d) Present Address: Department of Biochemistry, Wake Forest University, Winston-Salem, NC 27103. (e) University of California. (f) Present Address: Department of Chemistry, Princeton University, Princeton, NJ 08540.

(2) Malmstrom, B. G. *Annu. Rev. Biochem.* **1982**, *51*, 21–59.

(3) Eble, K. S.; Dawson, J. H. *Adv. Inorg. Bioinorg. Mech.* **1986**, *4*, 1–64.

(4) Poulos, T. G.; Finzel, B. C.; Gunsalus, I. C.; Wagner, G. C.; Kraut, J. *J. Biol. Chem.* **1985**, *260*, 16122–16130.

(5) (a) Hahn, J. E.; Hodgson, K. O.; Andersson, L. A.; Dawson, J. H. *J. Biol. Chem.* **1982**, *257*, 10934–10941. (b) Dawson, J. H.; Andersson, L. A.; Hodgson, K. O.; Hahn, J. E. In *Cytochrome P-450: Biochemistry, Biophysics, and Environmental Implications*; Heitanen, E., Laitinen, M., Hanninen, O., Eds.; Elsevier: Amsterdam, 1982; pp 589–596. (c) Dawson, J. H.; Andersson, L. A.; Davis, I. M.; Hahn, J. E. In *Biochemistry, Biophysics, and Regulation of Cytochrome P-450*; Gustafsson, J. A., Carlstead-Duke, J., Mode, A., Rafter, J., Eds.; Elsevier: Amsterdam, 1980; pp 565–572.

(6) Penner-Hahn, J. E.; McMurry, T.; Renner, M.; Latos-Grazynski, L.; Eble, K. S.; Davis, I. M.; Balch, A.; Groves, J. T.; Dawson, J. H.; Hodgson, K. O. *J. Biol. Chem.* **1983**, *258*, 12761–12764.

(7) Abbreviations: XAS, X-ray absorption spectroscopy; EXAFS, extended X-ray absorption fine structure; XANES, X-ray absorption near edge structure; EPR, electron paramagnetic resonance; ENDOR, electron-nuclear double resonance; HRP, horseradish peroxidase; TTP, dianion of 5,10,15,20-tetra-*m*-tolylporphyrin; TPP, dianion of 5,10,15,20-tetraphenylporphyrin; TMP, dianion of 5,10,15,20-tetramesitylporphyrin.

(8) Dunford, H. B.; Stillman, J. S. *Coord. Chem. Rev.* **1976**, *19*, 187–251.

(9) Hewson, W. D.; Hager, L. P. In *The Porphyrins*; Dolphin, D., Ed.; Academic: New York, 1979; Vol. 7, pp 295–332.

(10) Frew, J. E.; Jones, P. *Adv. Inorg. Bioinorg. Mech.* **1984**, *3*, 175.

(11) Yonetani, T.; Yamamoto, H.; Erman, J. E.; Leigh, J. S.; Reed, G. H. *J. Biol. Chem.* **1971**, *247*, 2447–2455.

(12) Mauk, M. R.; Girotii, A. W. *Biochemistry* **1974**, *13*, 1757–1763.

(13) Kobayashi, N.; Nozawa, T.; Hatano, M. *Biochim. Biophys. Acta* **1977**, *493*, 340–351.

(14) Theorell, H.; Ehrenberg, A. *Arch. Biochem. Biophys.* **1952**, *41*, 442–461.

(15) Dolphin D.; Forman, A.; Borg, D. C.; Fajer, J.; Felton, R. H. *Proc. Natl. Acad. Sci., U.S.A.* **1971**, *68*, 614–618.

(16) LaMar, G.; de Ropp, J. S.; Smith, K. M.; Langry, K. C. *J. Biol. Chem.* **1981**, *256*, 237–243.

(17) Roberts, J. E.; Hoffman, B. M.; Rutter, R.; Hager, L. P. *J. Biol. Chem.* **1981**, *256*, 2118–2121.

0002-7863/86/1508-7819$01.50/0

Scheme II

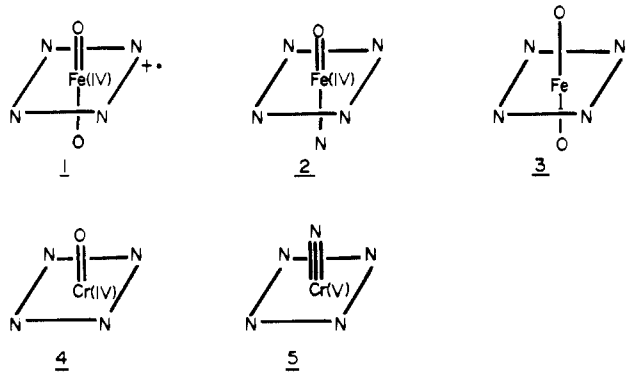

1 2 3 4 5

cation radical formulation. HRP-II is formed by one-electron reduction of HRP-I (Scheme I) and is therefore formally Fe^{IV}.[19,20] The Mössbauer spectra of HRP-I and HRP-II are very similar and are different from that of the ferric enzyme,[21,22] supporting the assignment of Fe^{IV} for both of the oxidized compounds.

Isotopic labeling studies have shown unequivocally that HRP-I and HRP-II contain one atom of oxygen,[23,24] but the protonation state of this oxygen has been a matter of controversy. HRP-I is generally believed to contain an oxo (double bonded oxygen) ligand, an assignment which is supported by ^{17}O ENDOR measurements.[25] Both oxo and hydroxyl ligation have been proposed for HRP-II; however, recent NMR[26] and resonance Raman[27] studies appear to be consistent only with the oxo assignment.

The site of oxidation for metalloporphyrins (i.e., metal centered vs. porphyrin centered) is quite sensitive to axial ligation.[28,29] Thus, the presence of Fe^{IV} rather than an Fe^{III} porphyrin π-cation in HRP-II indicates a strong ligand field. Although nitrido and carbido ligands[28] and dialkoxy ligation[30] are able to stabilize Fe^{IV} with respect to an Fe^{III} porphyrin π-cation, IEH calculations[31] suggest that an oxo ligand, but not a hydroxy ligand, is able to stabilize the Fe^{IV} configuration when the distal ligand is imidazole.

A straightforward method to characterize the axial ligation in HRP-I and HRP-II is via the structure of the Fe site. The instability of these species precludes X-ray diffraction studies; however, XAS is an ideal tool to investigate these structures. We have previously communicated[6] X-ray absorption near edge structure and preliminary extended X-ray absorption fine structure (EXAFS) results for HRP compounds I and II and related high-valent iron porphyrin model compounds. The first coordination environments of the Fe in these models (**1–3**) are illustrated in Scheme II. This work showed that both HRP species contain highly oxidized iron porphyrins (>Fe^{III}) and a coordination environment that can only be modeled by inclusion of a short (~1.6 Å) Fe–O interaction. A key feature of this work was the finding that HRP-I and HRP-II, and related compound I and compound II models, had identical structures from the perspective of XAS. At that time, we reported only preliminary results for the EXAFS analysis.

Recently, Chance et al. have reported the results of an XAS study of HRP-I, HRP-II, and related catalase complexes.[32] While confirming our results for HRP-I, this work suggested that HRP-II has a significantly different structure, characterized by a much longer (1.93 Å) Fe–O interaction. On the basis of this metric information, Chance et al. proposed a peroxidase mechanism involving formation of a double bonded (Fe=O) complex in HRP-I and, on reduction, a single bonded Fe–O complex in HRP-II. This mechanism is in conflict with findings from our laboratories[6] and with other evidence[21,22] that the Fe sites in HRP-I and HRP-II are very similar. In addition, this new mechanism, which would indicate hydroxyl ligation in HRP-II, contradicts a substantial body of evidence[26,27,31] favoring oxo ligation in this complex.

We report here the complete results of our EXAFS investigations of HRP-I and HRP-II. To improve the accuracy of our analysis, we have used K_2FeO_4 as a model for Fe=O EXAFS. Since the Fe–O distance in K_2FeO_4 is known to be quite short (1.67 Å),[33] this compound is a good model for determining the EXAFS parameters which characterize short Fe–O bonds, such as those which we have found in HRP-I and HRP-II. In order to test the validity of our data analysis procedure, we have obtained and analyzed XAS data for a crystallographically characterized high-valent oxo-chromium porphyrin that is thought to have a structure analogous to those of HRP-I and HRP-II. These results support our earlier[6] interpretation of the HRP-I and HRP-II structures and stand in contrast with those of Chance et al.[32]

Experimental Section

Sample Preparation and Handling. Commercial horseradish peroxidase (Type VI, Sigma) was further purfied by using the methods of Shannon et al.[34] to A_{403}/A_{275} greater than 3.56.[35] Highly concentrated (>5 mM) samples of HRP-I and HRP-II were generated[8] at ca. 0 °C in 5 mM potassium phosphate buffer (pH 7.0). Samples were prepared in the EXAFS sample cells (2 × 4 × 25 mm Mylar[36] windowed Lucite[36] frames) immediately prior to XAS data collection. HRP-I was prepared by addition of ethyl hydroperoxide to ferric HRP, giving a characteristic green solution. Addition of 1 equiv of reductant (ascorbate) to HRP-I resulted in formation of a red solution, characteristic of HRP-II. Sample composition was verified with UV–vis absorption spectroscopy at 4 °C on a diluted aliquot. By the UV–vis criterion, sample homogeneity was greater than 95% for both HRP-I and HRP-II. After preparation, the samples were frozen and maintained at −80 °C throughout data collection. Following completion of XAS data collection, the protein samples were immediately reanalyzed by UV–vis absorption spectroscopy; no significant degradation in sample homogeneity was observed.

High-valent iron porphyrin model compounds with formal oxidation states Fe^{IV} and Fe^{V} (see Scheme II) were prepared according to literature procedures. Complex **2**, (*N*-MeIm)(TTP)Fe^{IV}(O), is a formally Fe^{IV} model for the Fe site in HRP-II. It was prepared as previously described[37,38] by cleavage of a μ-peroxo porphyrin dimer. Complex **2** has a magnetic moment of 2.8 μ_B[38] and its electronic,[38] ^1H NMR,[38,39] and Mössbauer spectra[40] all show close similarities to the corresponding spectra of HRP-II. All of this evidence is consistent with a six-coordinate Fe^{IV} porphyrin having axial imidazole and oxo ligation.

The formally Fe^{V} models were prepared by oxidation of ferric porphyrins, with the two-electron oxidation of (TMP)Fe^{III} giving two dif-

(18) Hanson, L. K.; Chang, C. K.; Davis, M. S.; Fajer, J. *J. Am. Chem. Soc.* **1981**, *103*, 663–670.
(19) Hewson, W. D.; Hager, L. P. *J. Biol. Chem.* **1979**, *254*, 3182–3186.
(20) Hayashi, Y.; Yamazaki, I. *J. Biol. Chem.* **1979**, *254*, 9101–9106.
(21) Schulz, C. E.; Devaney, P. W.; Winkler, H.; Debrunner, P. G.; Doan, N.; Chiang, R.; Rutter, R.; Hager, L. P. *FEBS Lett.* **1979**, *103*, 102–105.
(22) Moss, T. H.; Ehrenberg, A.; Bearden, A. J. *Biochemistry* **1969**, *8*, 4159–4162.
(23) Schonbaum, G. R.; Lo, S. *J. Biol. Chem.* **1972**, *247*, 3353–3360.
(24) Adediran, S. A.; Dunford, H. B. *Eur. J. Biochem.* **1983**, *132*, 147–150.
(25) Roberts, J. E.; Hoffman, B. M.; Rutter, R.; Hager, L. P. *J. Am. Chem. Soc.* **1981**, *103*, 7654–7656.
(26) LaMar, G. N.; de Ropp, J. S.; Latos-Grazynski, L.; Balch, A. L.; Johnson, R. B.; Smith, K. M.; Parish, D. W.; Cheng, R.-J. *J. Am. Chem. Soc.* **1983**, *105*, 782–787.
(27) Terner, J.; Sitter, A. J.; Reczek, C. M. *Biochim. Biophys. Acta* **1985**, *828*, 73–80.
(28) English, D. R.; Hendrickson, D. N.; Suslick, K. S. *Inorg. Chem.* **1983**, *22*, 368–370.
(29) English, D. R.; Hendrickson, D. N.; Suslick, K. S. *Inorg. Chem.* **1985**, *24*, 122–127.
(30) (a) Groves, J. T.; Quinn, R.; McMurry, T. J.; Nakamura, M.; Lang, G.; Boso, B. *J. Am. Chem. Soc.* **1985**, *107*, 354–360. (b) Groves, J. T.; Gilbert, J. A. *Inorg. Chem.* **1986**, *25*, 125–127.
(31) Hanson, L. K., personal communication.
(32) Chance, B.; Powers, L.; Ching, Y.; Poulos, T.; Schonbaum, G. R.; Yamazaki, I.; Paul, K. G. *Arch. Biochem. Biophys.* **1984**, *235*, 596–611.
(33) McGinnety, J. A. *Acta Crystallogr.* **1972**, *B28*, 2845–2852.
(34) Shannon, L. M.; Kay, E.; Lew, J. Y. *J. Biol. Chem.* **1966**, *241*, 2166–2172.
(35) Eble, K. S., Ph.D. Thesis, University of South Carolina, 1985.
(36) Mylar and Lucite are registered trademarks of E. I. du Pont de Nemours & Co., Inc.
(37) Chin, D. H.; LaMar, G. N.; Balch, A. L. *J. Am. Chem. Soc.* **1980**, *102*, 4344–4350.
(38) Chin, D. H.; Balch, A. L.; LaMar, G. N. *J. Am. Chem. Soc.* **1980**, *102*, 1446–1448.
(39) LaMar, G. N.; de Ropp, J. S.; Latos-Grazynski, L.; Balch, A. L.; Johnson, R. B.; Smith, K. M.; Parish, D. W.; Cheng, R.-J. *J. Am. Chem. Soc.* **1983**, *105*, 782–787.
(40) Simmoneaux, G.; Scholz, W. F.; Reed, C. A.; Lang, G. *Biochim. Biophys. Acta* **1982**, *716*, 1–7.

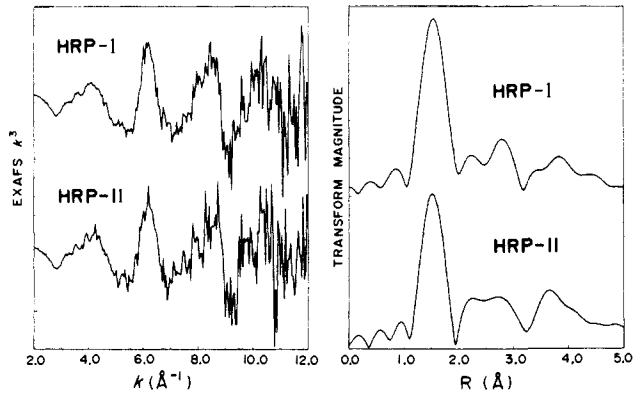

Figure 1. EXAFS spectra (left) and Fourier transforms (right) for HRP-I and HRP-II. EXAFS data are weighted by k^3 to enhance the amplitude of high k oscillations. EXAFS and Fourier transform calculated as described in text.

ferent high-valent model compounds.[41] In acidic solution, oxidation with *m*-chloroperoxybenzoic acid gave a green, HRP-I model (**1**) formulated as L(TMP$^+$)Fe^{IV}O.[41b,42] Under our conditions, L = methanol. The temperature and magnetic field dependence of the Mössbauer spectrum of **1** is indicative of an S = 1 Fe^{IV} that is strongly and isotropically coupled to an S = $^1/_2$ porphyrin π-cation.[42] Treatment of **1** with base, or oxidation of (TMP)Fe^{III} with iodosylbenzene, gave a different high-valent complex with a red color (**3**). On the basis of NMR and Mössbauer evidence,[30a] **3** is formulated as a bismethoxy complex of Fe^{IV}TMP. As a complement to the Fe studies, the crystallographically characterized[43-45] high-valent Cr porphyrins (TTP)Cr^{IV}O (**4**) and (TTP)Cr^{V}N (**5**) were also studied.

The high-valent Fe compounds (**1-3**) were examined as frozen toluene solutions while K_2FeO_4 and the Cr models (**4**, **5**, and K_2CrO_4) were prepared as powders diluted with BN and pressed into a thin pellet supported by mylar tape. The thermal lability of compounds **1-3** (rapid decomposition for temperatures above −80 °C) necessitated the development of new sample handling techniques. As described previously,[6] samples were prepared in polyethylene cells which permitted XAS and NMR spectra to be measured without the need for thawing and transferring the samples.

Data Collection and Reduction. X-ray absorption data were collected at the Stanford Synchrotron Radiation Laboratory on the wiggler beam line VII-3 and the focused beam line II-2, under dedicated running conditions (3-3.5 GeV, 40 mA, 8-pole wiggler field at 13 kG). The radiation was monochromatized with a Si(220) double-crystal monochromator. The data for the chromium compounds (**4**,**5**, and K_2CrO_4) were measured in transmission mode with nitrogen-filled ion chambers (2.0-cm gap, 300 V) to monitor incident and transmitted flux. The remaining data were collected as fluorescence excitation spectra with an array of Mn-filtered NaI(Tl) scintillation detectors to monitor the Fe Kα emission.[46] The data reported are an average of between 4 (for models) and 15 (for proteins) scans, comprising irradiation times of about 2-8 h/sample. Energy calibration was by the internal calibration technique,[47] using Fe and Cr foils, for Fe and Cr XAS respectively. Inflection points of the metal foil calibrations were assigned as 7111.3 eV (Fe) and 5988.8 eV (Cr).

The averaged data were reduced by subtracting a smooth polynomial pre-edge, extrapolated from a measured pre-edge; subtracting a two- or three-region cubic spline; and normalizing to the atomic falloff. The spline points were chosen empirically to minimize the residual low-frequency background while not reducing the observed amplitude of the EXAFS. The spline and its first and second derivatives were examined visually to ensure that the spline was not "fitting" the oscillatory component of the absorption. The normalized, background subtracted data were converted from energy E to photoelectron wave-vector $k = [2m(E - E_0/\hbar^2]^{1/2}$ with E_0 values of 7130 eV (Fe) and 6010 eV (Cr). Fourier transforms of the EXAFS data were calculated by numerical integration with k^3 weighted data. The EXAFS data and the corresponding Fourier transforms for HRP-I and HRP-II, for **1-3**, and for **4** and **5** are shown in Figures 1-3, respectively.

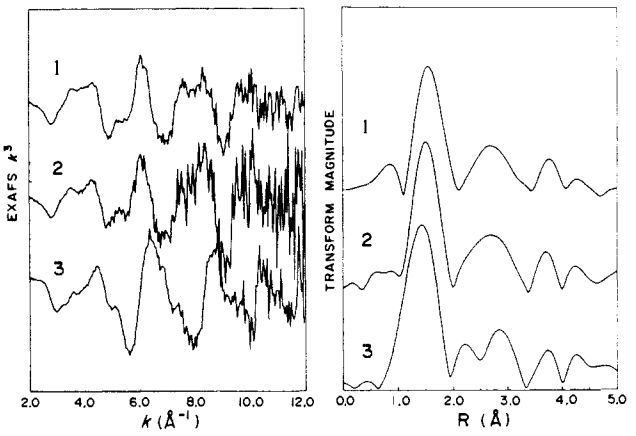

Figure 2. EXAFS spectra (left) and Fourier transforms (right) for **1**, **2**, and **3**. EXAFS data are weighted by k^3 to enhance the amplitude of high k oscillations. EXAFS and Fourier transform calculated as described in text. The EXAFS spectra show pronounced sensitivity to axial ligation, while the Fourier transforms show only a shift to lower R and a slight increase in peak width between **1** or **2** and **3** (see text).

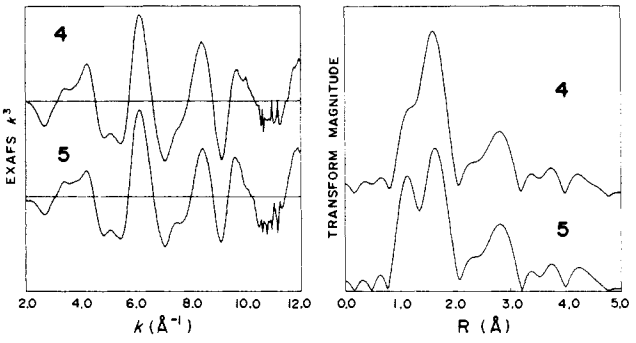

Figure 3. EXAFS spectra (left) and Fourier transforms (right) for **4** and **5**. EXAFS data are weighted by k^3 to enhance the amplitude of high k oscillations. EXAFS and Fourier transform calculated as described in text. The two principal peaks in the Fourier transform at $R \sim 1.5$ Å represent Cr=O (Cr≡N) and Cr—$N_{pyrrole}$, respectively.

Data Analysis

The observed EXAFS $\chi(k)$ can be expressed as

$$\chi(k) = \frac{\sum_i N_s F_s(k) e^{-2\sigma^2 k^2} e^{-2R_{as}/\lambda}}{kR_{as}^2} \sin [2kR_{as} + \phi_{as}(k)] \quad (1)$$

where N_s is the number of scatterers in the ith shell, F_s is the photoelectron backscattering amplitude of the ith shell, σ^2 is the mean-square variation in the absorber–scatterer distance, R_{as}, λ is the mean-free path length for the photoelectron, and $\phi_{as}(k)$ is the net phase shift in the photoelectron wave during scattering. The sum is taken over all shells of scatterers, where a shell consists of some number of indistinguishable atoms at the same (or indistinguishable) distance from the absorber. Typically, first shell bond lengths and coordination numbers can be determined to ±0.02 Å and ±20%, respectively.[48,49] In practice, differences of one or two in atomic number cannot be distinguished via EXAFS, thus a shell described below as nitrogen (N) could be due to C, N, or O. For two shells of the same atomic type, the approximate resolving power of EXAFS is $\Delta R \geq \pi/2k_{max}$.[49] Since k_{max} for

(41) (a) Groves, J. T.; Haushalter, R. C.; Nakamura, M.; Nemo, T. E.; Evans, B. J. *J. Am. Chem. Soc.* **1981**, *103*, 2884-2886. (b) Groves, J. T.; McMurry, T. J. *Rev. Port. Quim.* **1985**, *27*, 102-103.
(42) Boso, B.; Lang, G.; McMurry, T. J.; Groves, J. R. *J. Chem. Phys.* **1983**, *79*, 1122-1126.
(43) Groves, J. T.; Kruper, W. J., Jr.; Haushalter, R. C.; Butler, W. M. *Inorg. Chem.* **1982**, *21*, 1363-1368.
(44) Budge, J. R.; Gatehouse, B. M. K.; Nesbit, M. C.; West, B. O. *J. Chem. Soc., Chem. Commun.* **1981**, 370-371.
(45) Groves, J. T.; Takahashi, T.; Butler, W. M. *Inorg. Chem.* **1983**, *22*, 884-887.
(46) Cramer, W. P.; Scott, R. A. *Rev. Sci. Instrum.* **1981**, *52*, 395-399.
(47) Scott, R. A.; Hahn, J. E.; Doniach, S.; Freeman, H. C.; Hodgson, K. O. *J. Am. Chem. Soc.* **1982**, *104*, 5364-5369.
(48) Cramer, S. P.; Hodgson, K. O. *Prog. Inorg. Chem.* **1979**, *25*, 1-39.
(49) Lee, P. A.; Citrin, P. H.; Eisenberger, P.; Kincaid, B. M. *Rev. Mod. Phys.* **1981**, *53*, 769-806.

EXAFS data from dilute samples in typically 13–15 Å^{-1}, this places a lower limit of ~0.1 Å on the resolvable distance between shells; in practice, noise in the data results in an effective resolution closer to 0.2 Å.

Two different approaches were taken in the analysis of the EXAFS data. Both approaches involve determining the amplitude, $A_{as}(k)$, and phase, $\phi_{as}(k)$, which are expected for a particular absorber–scatterer interaction. The function $A_{as}(k)$ incorporates all of the factors which affect the amplitude, *except* N_s and R_{as}. As shown in eq 1, $A_{as}(k)$ depends on the identity of the absorber and the scatterers and on the length and strength of the absorber–scatterer bond. The phase shift of the photoelectron wave, ϕ_{as}, depends only on the identity of the absorber and the scatterer. Once determined, the functions $A_{as}(k)$ and $\phi_{as}(k)$ are used in conjunction with a nonlinear curve-fitting algorithm to model the observed EXAFS for an unknown compound. This approach makes use of the fact that amplitude and phase functions are reasonably transferrable form compound to compound,[49] *provided* that the chemical environments are similar.

It is possible to calculate ab initio the expected $A_{as}(k)$ and $\phi_{as}(k)$;[50] however, the calculated values generally require adjustment in order to correctly model experimental EXAFS.[49] This adjustment frequently takes the form of a linear scale factor, although more complicated functions are necessary to accurately reproduce the experimental data. In both of our analysis procedures, we have used experimental EXAFS of crystallographically characterized model compounds to empirically or semiempirically determine $A_{as}(k)$ and $\phi_{as}(k)$.

In the first method, a six-parameter function was fitted to the measured EXAFS for model compounds.[48] The models used were Fe^{II}(TPP) and Fe^{III}(TPP)(imidazole)$_2$ for Fe–N and K_2FeO_4 for Fe–O. This parametrized function was then used as a reference when fitting the EXAFS of unknown samples. When fitting unknowns, the number of scatterers and the absorber–scatterer distance were adjusted as variable parameters. The principal advantage of this approach is the small number of variable parameters per shell and the corresponding decrease in parameter correlation problems. Compared to the two variable parameters in the empirical approach,[48] some ab initio methods use as many as four variable parameters per shell[51] (scale factor, N_s, R_{as}, and σ_{as}). For multishell compounds (e.g., HRP-I) this can lead to parameter correlation problems. The primary difficulty with our empirical procedure is its limited flexibility, both in accurately reproducing the empirical $A_{as}(k)$ and $\phi_{as}(k)$ functions and in varying structural parameters when fitting unknowns.

The second analysis procedure was combination of empirical and semiempirical methods using a tabulated rather than a parametrized expression for the EXAFS amplitude and phase functions. These tabulated values permit more accurate reproduction of the details of the amplitude and phase functions. In the case of Fe–N EXAFS, ab initio amplitudes and phases[50] were used to fit the experimental Fe–N EXAFS from Fe^{II}(TPP). This fit gave the optimum values for a linear scale factor (0.34) and ΔE_0(−12 eV). In a procedure similar to Teo's FABM method,[52] the empirically optimized scale factor and E_0 were held fixed for all subsequent fitting. The values for the scale factor and ΔE_0 which were determined for Fe–N proved to be transferable to fitting of Cr–N EXAFS. When fitting unknown compounds, N_s was set at a chemically reasonable value (i.e., 4 or 5) and R_{as} and σ_{as} were optimized. Since σ_{as} is not known for our model compounds, the σ_{as} values determined in this way represent only the difference in σ_{as} between the model and the unknown.

This procedure was attempted for M–O EXAFS, using experimental EXAFS from K_2CrO_4 and K_2FeO_4.[53] In this case, however, it was not possible to obtain a good fit of the experimental data with the ab initio functions. The best fit was obtained for ΔE_0 = −20 eV, scale factor = 0.30, and σ_{as} = 0.0 Å. The reasons for the poor quality of this fit are apparent from a comparison of the empirical and theoretical values of $F_s(k)$. As shown in Figure 4, these functions have dramatically different shapes, which cannot be brought into agreement by means of a simple exponential factor. The reasons for this difference are unclear, although they may be related to the high oxidation state of the Fe and the strong bonding between the Fe and the O. The data in Figure 4 indicate that, when fitting data for compounds containing Fe=O bonds, the experimentally determined Fe—O amplitude function will probably give a more accurate fit than could be obtained with empirically adjusted ab initio parameters. The $A_{as}(k)$ and $\phi_{as}(k)$ functions for M–O EXAFS were determined from the experimental model compound EXAFS data with a Fourier back-transformation.[54] These functions were then used in the same manner as the ab initio functions, with ΔE_0 fixed at zero and the scale factor fixed at 1. As before, R_{as} and $\Delta\sigma_{as}$ were optimized when fitting unknowns.

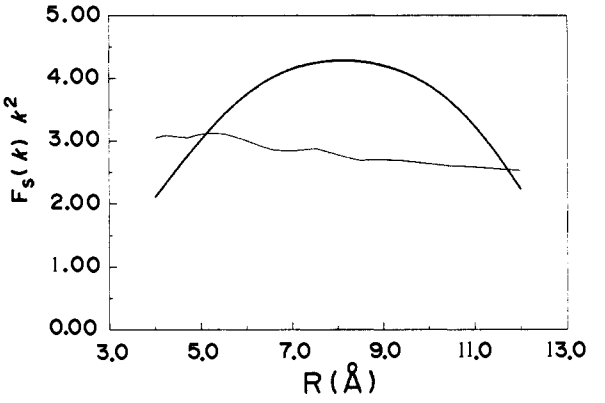

Figure 4. Empirical (heavy line) and theoretical (light line) amplitude functions $F_s(k)$ for Fe–O (see eq 1 for definition). Empirical $F_s(k)$ determined from complex back-transform of filtered first shell peak in Fourier transform of K_2FeO_4 EXAFS data. Theoretical function from ref 50. Theoretical function has been multiplied by the best fit scale factor (see text) of 0.30 to facilitate comparison. Amplitude functions multiplied by k^2 to approximately correct for k dependence of backscattering amplitude.

Results

As we have noted previously, the XANES spectra for HRP-I, HRP-II, **1**, and **2** are all extremely similar. In each case, the principal absorption discontinuity occurs at a higher energy than that found for Fe^{III} porphyrins. This suggests[6] the presence of Fe^{IV} in all four species. The spectra for HRP-I and HRP-II are superimposable within the noise level of the data, and those for **1** and **2** are quite similar.[6] These spectra all lack the intense pre-edge feature frequently associated with metal–oxo porphyrins; however, recent calculations[55] confirm that the XANES spectra for HRP-I, HRP-II, **1**, and **2** are consistent with an Fe^{IV}=O-(porphyrin) structure. The similarity of these XANES spectra demonstrates that the four different Fe sites must have similar structures.

This interpretation is supported by the previously noted[6] similarity in the EXAFS spectra of these compounds (Figure 1 and 2). The present work extends these qualitative observations to include the crystallographically characterized high-valent Cr porphyrins **4** and **5** (see Scheme II for structures). As shown in Figures 1–3, the EXAFS spectra for HRP-I, HRP-II, **1**, **2**, **4**, and **5** are all quite similar, with a characteristic principal maximum at $k \sim 6.1$ Å^{-1}. The EXAFS spectrum for **3**, with a maximum

(50) Teo, B.-K.; Lee, P. A. *J. Am. Chem. Soc.* **1979**, *101*, 2815–2832.
(51) See, for example: Antonio, M. R.; Teo, B.-K.; Cleland, W. E.; Averill, B. A. *J. Am. Chem. Soc.* **1983**, *105*, 3477–3484.
(52) Teo, B. K.; Antonio, M. R.; Averill, B. A. *J. Am. Chem. Soc.* **1983**, *105*, 3751–3762.
(53) Structural parameters for K_2CrO_4 and K_2FeO_4 and from Hoppe et al. (Hoppe, M. L.; Schlemper, E. O.; Murmann, R. K. *Acta Crystallogr.* **1982**, *B38*, 2237–2239) and from ref 33, respectively.
(54) Eisenberger, P.; Shulman, R. G.; Kincaid, B. M.; Brown, G. S.; Ogawa, S. *Nature (London)* **1978**, *274*, 30–34.
(55) Penner-Hahn, J. E.; Benfatto, M.; Hedman, B.; Takahashi, T.; Doniach, S.; Groves, J. T.; Hodgson, K. O. *Inorg. Chem.* **1986**, *25*, 2255–2259.

Table I. Iron–Porphyrin Structural Parameters[a]

	method I		method II		crystallography[b]	
sample	M–N[c]	M–O[c]	M–N[c]	M–O[c]	M–N[c]	M–O[c]
1	2.04	1.62–1.65	2.02	1.63–1.66		
2	2.02	1.64–1.65	2.03	1.65–1.66		
3	1.92		1.92			
4	2.01	1.51	2.01	1.52	2.03	1.57
5	2.02	1.49	*d*	*d*	2.04	1.57
HRP-I	1.99	1.61–1.62	2.00	1.62–1.64		
HRP-II	1.99	1.60	2.00	1.62–1.64		
6					2.005	1.604

[a] Metal to nearest-neighbor bond lengths from analysis of EXAFS data except as indicated. EXAFS results from nonlinear curve fitting methods described in text. M–N is the average $M–N_{pyrrole}$ bond length. For EXAFS results, the sixth ligand (methanol or imidazole) is included in this average. M–O is the M=O bond length or, for **5**, the Cr≡N bond length. [b] Crystallographic results from ref 32, 34, and 60. [c] M = Cr for **4** and **5**, Fe in all other cases. [d] Not determined.

at $k \sim 6.4$ Å^{-1}, is noticeably different over the range $k \sim 5$–9 Å^{-1}.

Despite these differences, all of the Fe EXAFS spectra give fairly similar Fourier transforms (Figures 1 and 2). The main peak in the transform for **3** is slightly broader and is shifted to slightly lower R relative to those for **1** and **2**; however, these differences are minor compared to the differences in the corresponding EXAFS spectra. This result illustrates the dangers of basing structural analyses on the simple qualitative appearance of the Fourier transform magnitudes. On the basis of a curve-fitting analysis (vide infra) the Fe porphyrins are found to contain two shells of ligands; however, these shells are not resolved in the Fourier transforms. In contrast, the Fourier transforms for the Cr porphyrins (Figure 3) show the presence of two distinct shells of nearest-neighbors. This is not surprising, since the Cr porphyrins are five-coordinate and thus are expected to have shorter Cr–(axial ligand) bond lengths and longer $Cr–N_{pyrrole}$ bond lengths than will be found in the six-coordinate Fe porphyrins. The curve-fitting analysis (vide infra) suggests that the inter-shell separation increases by 0.1 Å between the Fe and the Cr porphyrins. Evidently, this increase in separation is adequate to permit resolution of the two different shells in **4** and **5**. Note that despite the very different appearance of their Fourier transforms, the EXAFS spectra and structural parameters (vide infra) of **1**, **2**, **4**, and **5** are quite similar. This again illustrates that Fourier transforms cannot reliably be used to infer structural details.

The qualitative similarity in the EXAFS spectra for HRP-I, HRP-II, **1**, **2**, **4**, and **5** suggests that the structures of the metal sites in all of these species must be very similar. In order to test this interpretation, we have carried out a complete curve-fitting analysis of the EXAFS data. All of the results discussed below are based on data for which a Fourier filter has been used to isolate the EXAFS due to only those atoms in the first coordination sphere. This procedure greatly simplifies the analysis and in our hands gives no loss of accuracy. As a check, all final fits were repeated with unfiltered data. No change was observed in the structural results; however, the rate convergence for these fits was significantly slower. The quality of the fits was assessed by calculating the root-mean-square deviation between the data and the fit.

Chromium Model Compounds. Since they are structurally characterized,[43-45] the high-valent Cr compounds are useful for testing the accuracy of our data analysis procedures. Attempts to fit the first-shell EXAFS for **4** or **5** with a single shell of N atoms at ~2 Å gave poor agreement with the experimental data. The mean-square deviation between data and fit decreased by a factor of 2 on inclusion of a shell of O atoms at a short distance (1.5–1.6 Å). The final two shell fitting results for **4** and **5** are given in Table I.

Iron Complexes. The optimum paarameters for Fe–N and Fe–O were determined as described above. Fits were attempted with either one (N) or two (N + O) shells and with either four or five nitrogens in the nitrogen shell. The distances determined

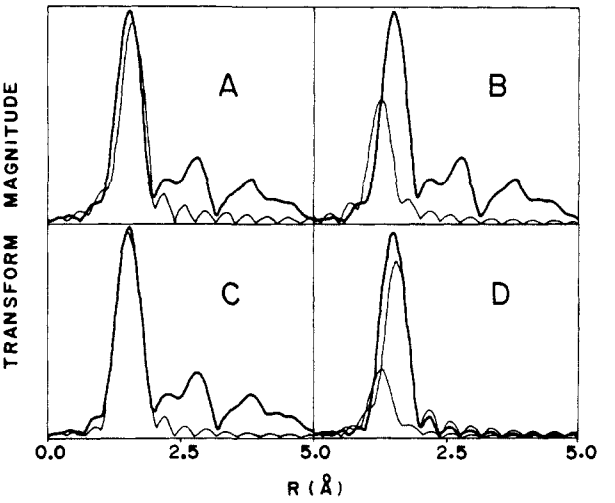

Figure 5. Fourier transforms of best fits to HRP-I data. Fits calculated with method I. Mean-square derivation, D, between data and fit given by $D = \{\sum[(\chi_{exp} - \chi_{fit})k^3]^2/(N-1)\}^{1/2}$. (A) HRP-I data (dark) and best fit (light) obtained when only a single shell of nitrogens (6.3 N at 1.99 Å, D = 1.2) was used. (B) HRP-I data (dark) and best fit (light) obtained when only a single shell of oxygen (1.9 O at 1.61 Å, D = 2.8) was used. (C) HRP-I dark (dark) and best fit (light) obtained when both a shell of nitrogen and a shell of oxygen (5.6 N at 1.99 Å; 1.1 O at 1.61 Å; D = 0.5) were used. (D) Best fit from two-shell fit (dark) and contributions from N and O shells. Note the absence of a resolvable Fe–O peak in the simulated data for two shells separated by 0.4 Å.

for these different fits were all very similar. The range of values reported in Table I represents the extreme values obtained for a particular distance in any of the different fits which were performed. The σ_{as} values determined in this way were quite sensitive to the details of the fit and in particular were strongly correlated to the number of scatterers used in the fit.

As noted above, the high-valent models **1** and **2** have essentially indistingusishable EXAFS spectra. These data could not be adequately fit with only a single shell of nitrogens. However, inclusion of a second shell of oxygen at ~1.6 Å decreased the mean-square deviation between data and the fit by a factor of 2 to 4. The results of these two-shell fits are given in Table I.

Essentially identical results were observed for HRP-I and HRP-II. These samples have nearly superimposable EXAFS spectra which cannot be fitted adequately with a single shell of atoms. In both cases, using either fitting method, the improvement in the mean-square deviation on inclusion of a second shell was at least a factor of 2. A typical set of fits, for HRP-I with method I, is shown in Figure 5. These fits demonstrate graphically the requirement of two shells in order to obtain a reasonable fit. As shown in Figure 5, the Fourier transforms for this range of data do not give resolvable peaks for the N at 2.0 Å and the O at 1.6 Å. Nevertheless, these shells can be resolved by curve-fitting methods. The quantitative curve-fitting results for HRP-I and HRP-II (Table I) are very similar to those obtained for their putative models **1** and **2**. This is consistent with the close similarity between the EXAFS spectra of the protein and those of the synthetic models (Figures 1 and 2).

The curve-fitting results for the high-valent model **3** were quite different from those of the other iron complexes. In this case, a reasonable fit was obtained with only a single shell of nitrogen, with a relatively short (1.92 Å) Fe–N. Attempts to improve this fit by including a shell of oxygen at a short distance resulted in the disappearance ($\sigma \rightarrow \sim 1$) of either the N or the O shell. These fitting results, together with X-ray edge spectra indicating a highly symmetric Fe environment,[6] are most consistent with a symmetric 6-coordinate structure having an *average* Fe–ligand distance of 1.92 Å. The Fe–N(porphyrin) distance expected for a 6-coordinate porphyrin is ~1.98 Å.[56] In order to obtain the observed average Fe–ligand distance, this would require an $Fe–O_{axial}$ distance of

(56) Scheidt, W. R.; Reed, C. A. *Chem. Rev.* **1981**, *81*, 543–555.

~1.80 Å in **3**. This interpretation is supported by recent NMR and Mössbauer data showing that **3** is in fact the bismethoxy adduct of Fe^{IV}(TMP).[30a] Analogous dialkoxy complexes of Cr[57] and Mn[58] porphyrins have average bond lengths of M–N = 2.01 Å and M–O = 1.84 Å, for an overall average M–ligand distance of 1.95 Å. These distances are consistent with the EXAFS results for **3**.

The EXAFS study of HRP reported by Chance et al.[32] included several fits in which shells separated by less than 0.1 Å were resolved (for example, HRP-II was reported to have Fe–N bond lengths of 2.10 and 2.00 Å and an Fe–O bond length of 1.93 Å). In our hands, attempts to fit multiple shells of the same atomic type (C, N, or O) suffer from severe parameter correlation. Nevertheless, we have attempted a similar fitting procedure for the data of **3**, in which we used two shells of N/O ligands at the appropriate distances (1.8 and 2.0 Å). Although it was possible to fit the data for **3** with shells located at ~1.85 and 1.98 Å, the improvement in the mean-square deviation for this fit relative to the single-shell fit was negligible (<10%). Thus we find, as expected for data to k_{max} = 13 $Å^{-1}$, that EXAFS cannot resolve the two shells of nearest neighbors which must be present in **3**.

Discussion

It is relatively difficult to analyze short (~1.6 Å) bond lengths via EXAFS since short bonds give only few EXAFS oscillations over the observable k range. In particular, we were concerned that the spline background removal procedure could introduce low-frequency artifacts which might resemble a short distance interaction. While such oscillations were observed for some three-region splines, no oscillations of the appropriate frequency were observed in the two-region splines used for this work. Therefore, this type of artifact cannot account for the 1.6-Å oxygen shell observed in the EXAFS data for HRP-I, HRP-II, **1**, and **2**. For compounds which have, or are thought to have, short M=O bond lengths, we observe a dramatic improvement in the quality of the fit when a 1.6-Å shell is included. No such improvement is observed for **3**, a complex that is thought *not* to have a short Fe–O bond.[30a] This provides additional evidence that the 1.6-Å shell is not an artifact of our analysis procedure.

The two different data analysis procedures give very similar results. Method I consistently gives bond lengths ~0.01 Å shorter than method II. This may reflect the fact that E_0 was not optimized for method I; however, the difference is smaller than the estimated uncertainty in the EXAFS. The curve-fitting results for **4** and **5** demonstrate that the accuracy of our data analysis procedure is ±0.02 Å for M–N bond lengths. The short M=O bond lengths in **4** and **5** seem to be underestimated by ~0.05 Å. If this result is applicable to the Fe system, it is necessary to add 0.05 Å to the Fe=O bond lengths given in Table I. We note, however, that in the Cr case, a more accurate fit was obtained if E_0 was made an adjustable parameter, while a similar fit for Fe did not give any change in the Fe=O bond length. This would suggest that the error for **4** and **5** is due to an error in E_0 and that the error in the Fe=O distance determination is less than 0.05 Å. Taking these factors into account, we estimate an uncertainty of ±0.03 Å in the M–O bond length determinations.

The most significant result of this work is the determination of the presence and length of the Fe–O bond in HRP-I and HRP-II and in their high-valent Fe porphyrin models. Our EXAFS results show that this distance is 1.64 ± 0.03 Å for all four postulated ferryl species. The corresponding Cr–O distance in the chromyl analogue **4**[43] and in oxo-Cr^{V}(salen) complexes[59] is 1.55–1.57 Å. An increase of ca. 0.08 Å in the M–O distance is completely consistent[56] with the addition of two 3d electrons in moving from Cr^{IV} to Fe^{IV}. For example, in **1**[42] these electrons are added to the (d_{xz},d_{yz}) orbitals and thus should cause a noticeable lengthening of the M–O bond. More direct support for our proposed structures is found in the recent preparation and

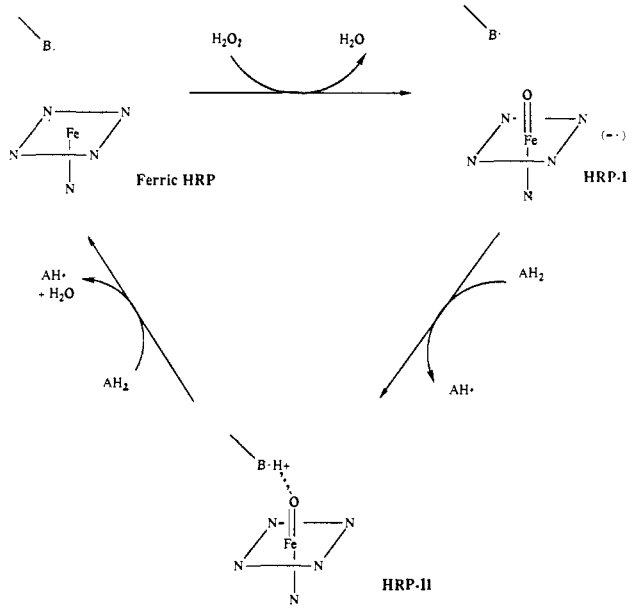

Figure 6. Catalytic scheme for HRP consistent with results of EXAFS analysis. Only the immediate coordination environment of the Fe is shown; protoporphyrin IX is indicated schematically by a parallelogram with N at the vertices, and only one nitrogen atom from the distal imidazole is indicated. Fe–ligand bond lengths are given in Table I. The ionizable amino acid residue (possibly imidazole) is indicated as B.

preliminary structural characterization of a new HRP-II model, Fe^{IV}(O)(THF)(TPivP),[60] **6**. Although this structure suffers from disorder, it indicates that the ferryl Fe=O bond length is 1.604 ± 0.019 Å.[58] The bond length increase of 0.04 Å between **6** and HRP-I or HRP-II is only marginally significant; however, this may reflect the greater strength of the distal Fe–N(imidazole) bond in HRP relative to the Fe–O(THF) bond in **6**. Our structural results for HRP-I and HRP-II are consistent only with a double bonded ferryl (Fe=O) structure, and not with a single bonded hydroxyl (Fe—O) structure.

We also find that the structures of HRP-I and HRP-II, and the corresponding models (**1** and **2**, respectively), are indistinguishable from an EXAFS perspective. This confirms that the model compounds are in fact good *structural* models of the enzyme active site. There are small differences in the X-ray absorption edge structure of the enzyme and the models,[6] but these clearly do not represent significant structural variations.

Our finding that HRP-I and HRP-II are very similar structurally is at odds with the findings of Chance et al.,[32] who suggest that HRP-II has a much longer, 1.93 Å, Fe–O single bond. The two proposed structures for HRP-I are very similar, thus ruling out different data analysis procedures as accounting for the discrepancy in HRP-II structures. We note that the EXAFS spectra for HRP-I and HRP-II shown in Figure 4 of ref 32 are noticeably different, in contrast to the similarity which we observe (Figure 1). The reasons for this difference remain to be resolved; however, we note that our results are consistent with the suggestion (vide supra) that the principal difference between HRP-I and HRP-II is the presence of a porphyrin π-cation in the former. In particular, the similarity of the Mössbauer spectra[21,22] and the X-ray absorption edge spectra[6] of HRP-I and HRP-II suggests that the Fe environment in the protein forms must be very similar. Finally we note that the only high-valent Fe porphyrin complex to have been crystallographically characterized (complex **6**, above) is in fact a model for HRP-II,[60] The Fe–O bond length in **6** is consistent with our results and inconsistent with those of Chance et al.

The reduction of HRP-I is known to occur with concomitant uptake of one proton;[8-10] however, our results show that this does not result in protonation of the oxo ligand. This is not surprising,

(57) Haushalter, R. C.; Groves, J. T., unpublished results.
(58) Camenzind, M. J.; Hollander, F. J.; Hill, C. L. *Inorg. Chem.* **1982**, *21*, 4301–4308.
(59) Srinivasan, K.; Kochi, J. *Inorg. Chem.* **1985**, *24*, 4671–4679.
(60) Schappacher, M.; Weiss, R.; Montiel-Montoya, R.; Trautwein, A.; Tabard, A.; Tabard, A. *J. Am. Chem. Soc.* **1985**, *107*, 3736–3738.

since the Fe^{IV}=O moiety is unlikely to be a strong base. A possible location for this added proton is suggested by recent resonance Raman results,[61] which indicate the presence of an ionizable group (probably imidazole) within hydrogen-bonding distance of the oxo ligand. A proton in this location would then be available when HRP-II is converted, with the uptake of an electron and a second proton, to ferric HRP and water (Figure 6).[62a] The fact that HRP-I and HRP-II have similar iron-site structures may facilitate rapid reduction of HRP-I during the catalytic cycle, since there would be only a small reorganizational energy barrier to this reaction. The apparently pervasive nature of short Fe=O bonds in high-valent Fe porphyrins (HRP-I, HRP-II, **1**, and **2**),[62b] together with the similar reactivity of HRP and P-450 on treatment with peroxide, suggests that a similar ferryl (Fe=O) complex may be the active oxygen species in P-450.

Acknowledgment. This work was supported by the National Science Foundation (CHE 85-08115 to K.O.H., CHE 84-06373 to J.T.G., and DMB 86:05876 to J.H.D.), the National Institutes of Health (GM 26226 to A.L.B.) and a Camille and Henry Dreyfus Distinguished Young Faculty Award (to J.E.P.H.). J.H.D. is a Camille and Henry Dreyfus Teacher/Scholar, an Alfred P. Sloan Research Fellow, and a recipient of a National Institutes of Health Research and Career Development Award (AM-01123). Synchrotron radiation was provided by the Stanford Synchrotron Radiation Laboratory which is supported by the United States Department of Energy and the National Institutes of Health through the Biotechnology Resource Program in the Division of Research Resources. We wish to thank Dr. S. P. Cramer for the loan of NaI(Tl) scintillation detectors, Professor R. A. Scott for the gift of data analysis software, Dr. Dennis Koop for helpful suggestions concerning the purification and handling of horseradish peroxidase, and Ian M. Davis for experimental assistance.

Registry No. 1, 95724-73-5; **2**, 73133-16-1; **3**, 93862-19-2; **4**, 80584-26-5; **5**, 84192-46-1; **6**, 96482-28-9; Fe, 7439-89-6; Cr, 7440-47-3; O_2, 7782-44-7; N_2, 7727-37-9; peroxidase, 9003-99-0; heme, 14875-96-8.

Supplementary Material Available: A listing of X-ray absorption vs. energy for the spectra reported herein (34 pages). Ordering information is given on any current masthead page.

(61) Sitter, A. J.; Reczek, C. M.; Terner, J. *J. Biol. Chem.* **1985**, *260*, 7515-7522.

(62) **Notes Added in Proof.** (a) A similar compound II reduction mechanism has recently been proposed by Makino et al. (Makino, R.; Uno, T.; Nishimura, Y.; Iizuka, T.; Tsuboi, M.; Ishimura, Y. *J. Biol. Chem.* **1986**, *261*, 8376-8382) on the basis of variable pH resonance Raman measurements. (b) Additional examples of short Fe-O bonds have recently been reported by M. Chance et al. for ferryl myoglobin (Chance, M.; Powers, L.; Kumar, C.; Chance, B. *Biochemistry*, **1986**, *25*, 1259-1266) and cytochrome *c* peroxidase compound ES (Chance, M.; Powers, L.; Poulos, T.; Chance, B. *Biochemistry*, **1986**, *25*, 1266-1270). This new evidence provides further support for our finding that the Fe=O moiety is a common structural feature of high-valent iron porphyrins.

Single Crystal Neutron Diffraction Refinement of Bullvalene at 110 K

P. Luger,*† J. Buschmann,† R. K. McMullan,‡ J. R. Ruble,§ P. Matias,§ and G. A. Jeffrey§⊥

Contribution from the Institut für Kristallographie, Freie Universität Berlin, D-1000 Berlin 33, Federal Republic of Germany, the Chemistry Department, Brookhaven National Laboratory, Upton, New York 11973, and the Department of Crystallography, University of Pittsburgh, Pittsburgh, Pennsylvania 15260. *Received May 27, 1986*

Abstract: A low-temperature neutron diffraction refinement of the crystal structure of bullvalene, $C_{10}H_{10}$, tricyclo-[3.3.2.0^{2,8}]deca-2,5,8-triene, shows that the molecule is distorted only very slightly from the C_{3v} symmetry expected for the isolated molecule, although the crystal structure symmetry is monoclinic. There is a small but significant difference between the shortest and longest of the C-C bonds in the cyclopropane ring, which are 1.536 (1), 1.533 (1), and 1.530 (1) Å. The three ethylenic wings of the molecule are virtually identical, except for small differences in planarity and C-C-H angles. One wing is exactly planar within 0.002 (3) Å. In the other two, one of the hydrogen atoms in each is significantly displaced from the plane by 0.027 (3) and 0.023 (3) Å. The mean bond lengths in the ethylenic wings are C_{ring}—C, 1.4727 (7) Å; C=C, 1.3423 (7) Å; =C—C, 1.5163 (7)Å. The C-H bond lengths range from 1.086 (2) to 1.092 (2) Å. The thermal motion analysis gives an unusually good fit to the rigid-body model. Corrections for harmonic thermal motion lengthened all C—C and C=C bonds uniformly by 0.003 Å. For the C-H bonds, the harmonic riding motion and anharmonicity corrections almost cancel, so that the thermally corrected bond lengths differ from those measured by ±0.001 Å.

Bullvalene attracted much interest when first synthesized[1] 23 years ago because of the interesting chemistry involved.[2] This prompted X-ray structure analyses of first some bullvalene $AgBF_4$ complexes[3] and then of bullvalene itself.[4,5] The solid-state ^1H NMR shows an unusual decrease in line width with increase of temperature at about 20 °C, which was attributed either to valence bond isomerism or molecular reorientation.[6] The room temperature X-ray analysis provided no evidence in support of the valence isomerism hypothesis, and the NMR results were interpreted as due to the onset of molecular motion leading to the

† Freie Universität Berlin.
‡ Brookhaven National Laboratory.
§ University of Pittsburgh: Research Collaborators at Brookhaven National Laboratory.
⊥ A. von Humboldt U.S. Senior Scientist Awardee.

(1) Schröder, G. *Angew. Chem., Int. Ed. Engl.* **1963**, *2*, 481-482.
(2) Doering, W. E. von; Roth, W. R. *Tetrahedron* **1963**, *19*, 715-737.
(3) McKechnie, J. S.; Newton, M. G.; Paul, I. C. *J. Am. Chem. Soc.* **1967**, *89*, 4819-4825.
(4) Johnson, S. M.; McKechnie, J. S.; Lin, B. T.-S.; Paul, I. C. *J. Am. Chem. Soc.* **1967**, *89*, 7123.
(5) Amit, A.; Huber, R.; Hoppe, W. *Acta Crystallogr., Sect. B: Struct. Crystallogr. Cryst. Chem.* **1968**, *B24*, 865-869.
(6) Graham, J. D.; Santee, E. R., Jr. *J. Am. Chem. Soc.* **1966**, *88*, 3453-3454.

0002-7863/86/1508-7825$01.50/0